

EXPERIMENTAL STUDIES OF ASEISMIC PROPERTIES OF VARIOUS TYPE WATER TANKS

CHIKAHIRO MINOWA

SUMMARY

Several plastic-made water tanks of various configurations were tested by using the shaking tables to study the effects of contained water during earthquakes. The configurations included the up-lift circular cylinders, sphere and rectangle. The results of shaking table tests of circular cylindrical tanks were compared with the analysis of assumed mode methods considering the bulgings, the sloshings and the rocking of base frame. From the results of spherical water tank tests, the coefficients which were necessary to the rocking analysis of spherical water tanks were estimated. The nonlinear sloshing analysis of rectangular water tanks to earthquake motions was calculated.

INTRODUCTION

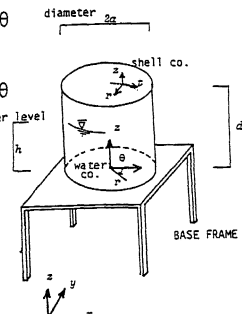
In recent earthquakes, many water tanks installed in buildings leaked from side walls or pipe connections. Furthermore, some water tanks were collapsed, and the contained water ran down the stairs. This water made troubles to electric power systems, and should be dangerous to evacuations. Besides, the water is necessary in earthquake disasters. In this meaning, it is important to make the water tanks strong to earthquakes.

Many researches about the aseismic properties of liquid fuel tanks have been carried down. However, the investigations for water tanks are scarce. In this paper, the dynamic characteristics about the water tanks of three configurations, that is, circular cylinder, sphere and rectangle, are investigated experimental and compared with computer analyses.

CIRCULAR CYLINDRICAL WATER TANK

Two shaking table test results are presented. One is the test of actual water tank which is made of fiber reinforced plastics(FRP), and which is mounted on the high-rise steel frame. The other is the test of model tank which is made of clear vinyl chlorides. The assumed mode methods are applied to the theoretical analyses of these tanks. In these analyses, the circular cylindrical tank is assumed to be supported with an elastic base frame. The base frame may be expressed by rocking and sway springs in mathematical models. The model and coordinates are shown in Fig.1. The displacements in the radial(r), tangential(θ), and axial(z) directions are represented by u_r , u_θ , and u_z respectively. These displacements are defined as follows.

Research Engineer, National Research Center for Disaster Prevention,
Tsukuba, Japan

$$\begin{aligned}
u_r &= (u_g + u_o - (H+z)\psi) \cos \theta + \sum_p \sum_q \zeta_{pq} r f_{pq}(z) \cos q\theta \\
u_\theta &= (u_g + u_o - (H+z)\psi) \sin \theta + \sum_p \sum_q \xi_{pq} \theta f_{pq}(z) \sin q\theta \\
u_z &= a \psi \cos \theta + \sum_p \sum_q \eta_{pq} z f_{pq}(z) \cos q\theta \quad \dots \text{Eqs. (1)}
\end{aligned}$$


ANALYTICAL MODEL OF
CIRCULAR CYLINDRICAL WATER TANKS
Fig.1

where u_g is the input displacement in the X-direction, u_o is the deformation of base frames, ψ is the angle of rotations, H is the position of a rocking center, q is the circumferential wave number, $r f_{pq}(z)$, $\theta f_{pq}(z)$, $z f_{pq}(z)$ are the assumed functions in the r -, θ -, and z -direction respectively, ζ_{pq} , ξ_{pq} , and η_{pq} are the generalized coordinates in the r -, θ -, and z -direction respectively. Waters are assumed to be ideal fluids. Using Bessel and modified Bessel functions $J_m(r)$, $I_n(r)$, the velocity potential ϕ is expressed as follow.

$$\begin{aligned}
\dot{\phi} &= -(\dot{u}_g + \dot{u}_o - (H+z)\dot{\psi}) r \cos \theta + \sum_l \sum_m \dot{A}_{lm} J_m(\alpha_{lm} r) \cosh \alpha_{lm} z \cos m\theta \\
&\quad + \sum_k \sum_n \dot{B}_{kn} I_n\left(\frac{k\pi}{2h} r\right) \cos \frac{k\pi}{2h} z \cos n\theta \quad \dots \text{Eq. (2)}
\end{aligned}$$

where α_{lm} satisfies $J'_m(\alpha_{lm}) = 0$. In order to complete the rotational solutions, the expansions in Bessel functions are necessary in addition to the elementary solution (Ref. 1). However, only the elementary solution is applied to this analysis for conveniences. The motions of shell walls and waters are assumed to continue in the r -direction, so that B_{kn} is expressed by the series of ζ_{pn} . Substituting total potential energies and total kinetic energies into Lagrange's equations, the equations of tank motions are obtained. Following functions are used for assumed functions, in the case of roof cuts, for $q=0,1,2,3,\dots$

$$r f_{pq}(z) = \sin \frac{p\pi}{2d} z, \quad \theta f_{pq}(z) = \sin \frac{p\pi}{2d} z, \quad z f_{pq}(z) = \sin \frac{p\pi}{2d} z, \quad p=1,3,\dots$$

in the case of roof caps,

$$\text{for } q=1, \quad r f_{pq}(z) = \sin \frac{p\pi}{2d} z, \quad \theta f_{pq}(z) = \sin \frac{p\pi}{2d} z, \quad z f_{pq}(z) = \sin \frac{p\pi}{2d} z, \quad p=1,3,\dots$$

$$\text{for } q \neq 1, \quad r f_{pq}(z) = \sin \frac{p\pi}{d} z, \quad \theta f_{pq}(z) = \sin \frac{p\pi}{d} z, \quad z f_{pq}(z) = \sin \frac{p\pi}{d} z, \quad p=1,2,\dots$$

The roof restrained condition for circumferential modes of $\cos \theta$ may be given by $\sum_p \zeta_{p1} \sin \frac{p\pi}{2} = \sum_p \xi_{p1} \sin \frac{p\pi}{2}$. Assuming $\zeta_{pq} = \xi_{pq}$, this condition is satisfied. Besides, the roof will be represented by a shell element with high rigidities approximately.

Elevated tank test

The circular cylindrical water tank mounted on a steel frame shown in Fig.2 was tested by using the shaking table. This tank was manufactured from FRP, and capped with a roof. This tank didn't possess the complete circular cylinder, but the radius of roof sections was slightly smaller than that of base sections. The

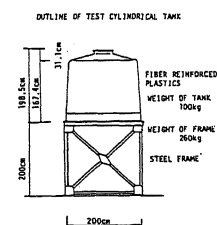


Fig.2

mean radius was about 95cm. The thickness of a shell wall wasn't uniform in the reason of man-made productions. This thickness was about 3.5mm. This tank was anchored in the steel frame 8 bolts at 45° intervals. According to the measured mode in Fig.3, the tank mounted on a brace frame was considered to undergo rocking vibrations. These rocking vibrations were generated by the total bending in a brace frame, and by the extensions of anchor bolt connections. The rocking center of this system was estimated to locate about 50cm under the base plate of tank. Fig.4 shows the relations between natural frequencies and water levels. The values of frame springs were evaluated by the natural frequency of the empty tank test. The natural frequencies of the tank on a brace frame were calculated in two cases. One was a rotational spring only, the other was a sway spring only. The rotatory inertia of a frame was assumed to be 1037 kg.cm.sec². The tank supported by a frame without braces was tested, and the measured natural frequencies were coincided with calculations.

Model tank test

The shaking table test of a model tank which was manufactured of vinyl chlorides, shown in Fig.5, were carried out in two cases of roof caps and roof cuts. The well-known out-of-round deformations were observed. When a shell wall is strengthened with J numbers of vertical ribs in equal intervals, the circumferential modes of $J \times I \pm 1$ wave numbers ($I=0,1,2,\dots$) may be excited. As vertical ribs were attached at two positions parallel to the shaking direction, the circumferential modes of odd wave numbers may be excited. However, the values of participation factors except for $\cos \theta$ modes were calculated very small. Fig.6 shows the strain circumferential distribution for two roof cases. The test results were compared with analyses for the water level of 80%. The distributions of 6Hz in the roof cut case and those of 8Hz in the roof capped case were $\cos 5\theta$ modes, those

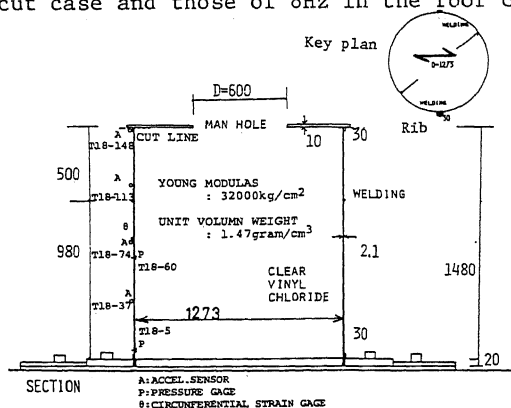


Fig.5

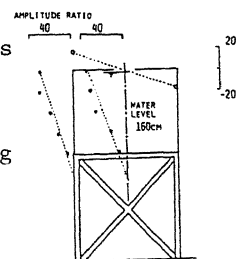


Fig.3

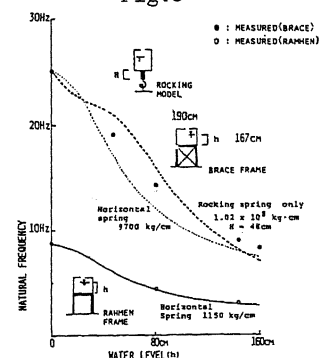


Fig.4

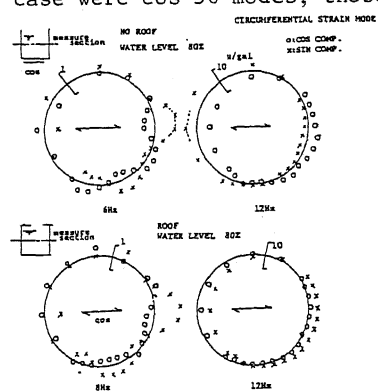


Fig.6

of 12Hz excitations in two roof conditions were $\cos \theta$ modes. The relations between natural frequencies and circumferential wave numbers are shown in Fig.7 and 8 for two roof cases. The analyses considering static stresses(Ref. 2) would give good agreements with test results. Fig.9 shows the vertical distributions of $\cos 5\theta$ modes.

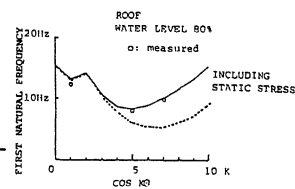


Fig.7

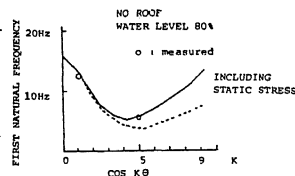


Fig.8

The roof effects on $\cos \theta$ modes were investigated. In low water levels that the influence of a roof mass was larger in comparison with water mass, the natural frequencies of the roof capped case would be measured lower than those of the roof cut case. In high water levels that the influence of a roof mass was small, the differences in natural frequencies between two roof cases were supposed to be scarce. Judging from the impulse response records of water levels 80% and 100% shown in Fig.10, the roof capped case showed slightly higher frequencies. In the analyses of $\cos \theta$ modes, in order to agree with test results, the rotational spring was assumed to be $k_\psi = 7 \times 10^7 \text{ kg} \cdot \text{cm}$. The roof cut case of water level 80% gave natural frequency of 12.2Hz in analyses. The roof capped case of the same water

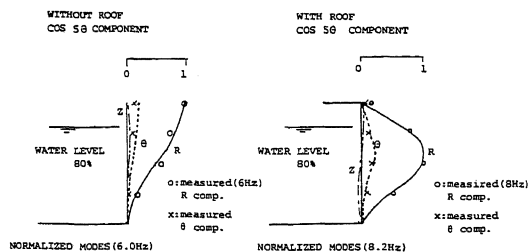


Fig.9

level gave 13.2Hz, assuming $\zeta_{p1} = \xi_{p1}$ in Eqs.(1). However, using the conditions of $\zeta_{p1} = \xi_{p1}$, circumferential strains were never found. The approximate analyses assuming that a roof was a thick shell element, gave a natural frequency of 12.4Hz for the thickness of 20cm, and 13.2Hz for that of 40cm. Fig.11 shows the vertical distributions for two roof cases.

The roof cut tank of water level 90% was tried to be destroyed dynamically. The dynamic characteristics of this tank was shown in Fig.12. The circumferential mode of a peak frequency 10.5Hz was $\cos \theta$ mode. The vertical distributions of strains, water pressures and deformations at

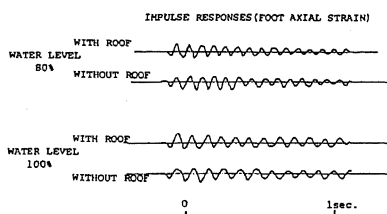


Fig.10

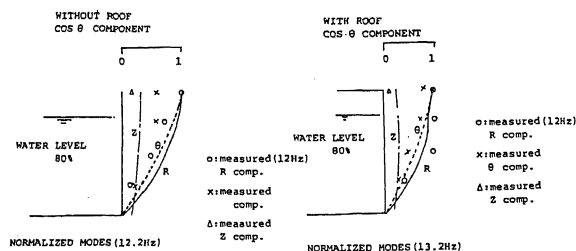


Fig.11

this frequency are shown in Fig.13. The shaking table excited this tank in this frequency with amplitudes of 2G, in a short rise time. The collapse occurred in a moment. Measured response waves and calculated response waves are shown in Fig.15. The response waves were made straight lines from the time point that cracks of walls were estimated to break out. The time histories of vertical distributions for measured accelerations and integrated displacements, and those of circumferential strain distributions are shown in Fig.14. A time point 0.10sec. in Fig.14 corresponded to the start time of straight lines in Fig.15. Video records in Photo 1 shows crack spreads. The position where a crack broke out, was estimated to be a little higher than half heights of the tank. This position corresponded to the peak of water pressure distributions. This excitations were considered to be impulsive. The materials of a tank; vinyl chlorides were fragile to impulsive forces, so that this tank collapsed in small strains. Circumferential strains about 800×10^{-6} measured near at positions where cracks broke out.

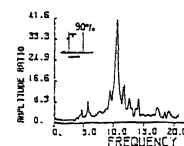


Fig.12

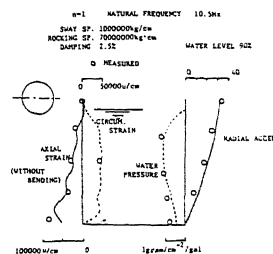


Fig.13

g : Circumferential strain
(M) : Measure
(C) : Computer Simulation

SENSOR	MAXIMUM	
T18-74θ(M)	1313.8	$\times 10^{-6}$
T18-74θ(C)	1030.2	$\times 10^{-6}$
T18-148 (M)	3032.3	GAL
T18-148 (C)	3267.7	GAL
T18-113 (M)	2333.2	GAL
T18-113 (C)	3014.4	GAL
T18-74 (M)	1961.3	GAL
T18-74 (C)	2236.2	GAL
T18-37 (M)	1777.1	GAL
T18-37 (C)	1364.1	GAL
T18-60 (M)	124.3	GRAM/CH ²
T18-60 (C)	119.3	GRAM/CH ²
T18-3 (M)	130.1	GRAM/CH ²
T18-3 (C)	111.9	GRAM/CH ²
TABLE-A	2666.6	GAL (input)
TABLE-D	4620.0	MICRON

DAMPING 20% FOR FIRST MODE.

COLLAPSE TEST. WATER LEVEL 135cm(90%)

Fig.15

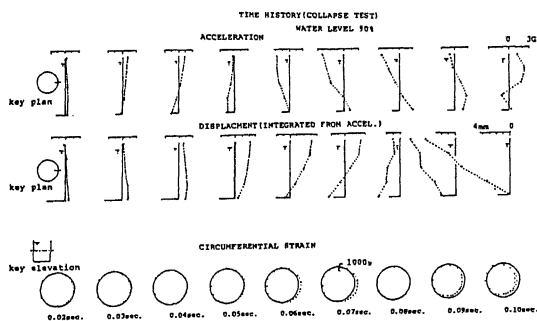


Fig.14

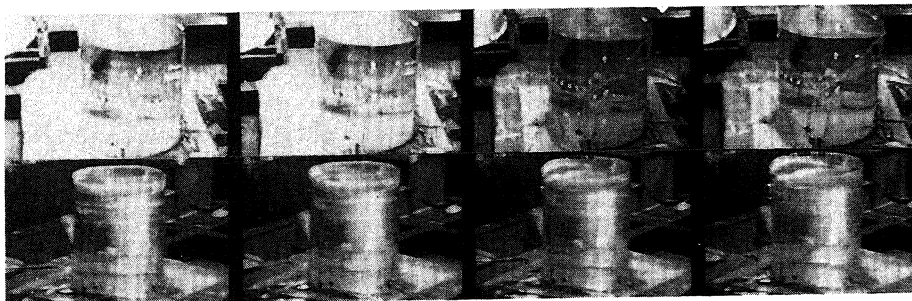


Photo 1. The intervals of frames are 1/60sec.
The first line superimposed in lower photos is table accel.

SPHERICAL WATER TANK TESTS

Spherical tanks are assumed to be rigid, so that the main purpose of analyses will be to obtain sloshing forces and effective masses of water. Many excellent researches for spherical tanks were already done. The FRP spherical water tank with capacities of 1 ~ 5 tons are seen to be mounted on steel frames in the roofs of buildings. These tanks are considered to undergo rocking motions during earthquakes. The FRP spherical water tank of 186cm in diameter, shown in Fig.18, was tested by using the shaking table. The dominant frequencies which were measured for each water level, are indicated in Table 1. These dominant frequencies were coincided with available theories(Ref. 3). The horizontal spring was estimated from the dominant frequency of an empty tank. However, according to Fig.17, this tank underwent rocking motions. The rocking center was estimated to locate in the vicinity under a tank base.

The rocking equation of spherical tanks in high frequency ranges comparing with first sloshing frequency, and considering only an elementary solution of rocking waters, is obtained as follow, and the model is shown in Fig.16,

$$H(M_C + M_L(1 - z_0) - m_L(1 + \frac{Y}{H}))\ddot{u}_g + (I_G/H^2 + M_L(1 - \frac{z_0}{H})^2 + M_C + I_C/H^2 - m_L(1 + \frac{Y}{H})^2)H^2\ddot{\psi} + K_\psi\psi = 0 \quad \dots \text{Eq. (3)}$$

where M_C is the mass of spherical tank, M_L is the mass of contained water, m_L is the mass for sloshings after Shimizu(Ref. 4), I_C and I_L are rotatory inertias for spherical tank and contained water, respectively. The natural frequencies in low water levels indicated higher values than test results, because of using only an elementary solution of rocking waters. Considering that Y is a parameter Y_0 , this Y_0 will be evaluated from measured natural frequencies. Y_0 is indicated in Table 1. The rocking spring was estimated from the frequency of an empty tank. This spring would be decided by anchor bolt connections.

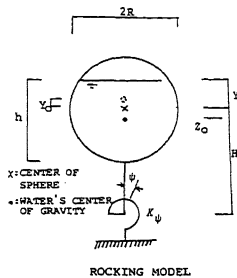


Fig.16

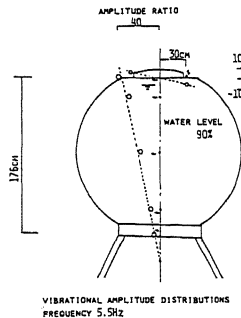


Fig.17

WATER LEVEL cm	h/2R	OBSERVED FREQUENCY	Y ₀ /2R
0	0	21.0Hz	
18.6	0.1	21.0Hz	-0.40
37.2	0.2	21.0Hz	-0.31
55.8	0.3	18.5Hz	-0.27
74.4	0.4	15.5Hz	-0.22
93.0	0.5	11.0Hz	-0.22
111.6	0.6	9.0Hz	-0.16
130.2	0.7	7.2Hz	-0.15
148.8	0.8	6.2Hz	-0.07
167.4	0.9	5.5Hz	0.07

Table 1

Frame mass: 0.128kg.sec²/cm

Frame moment of inertia: 80kg.cm.sec²

Tank mass: 0.09kg.sec²/cm

Tank moment of inertia: 513kg.cm.sec²

Rocking center: 25cm under a tank base

OUTLINE OF TEST SPHERICAL TANK

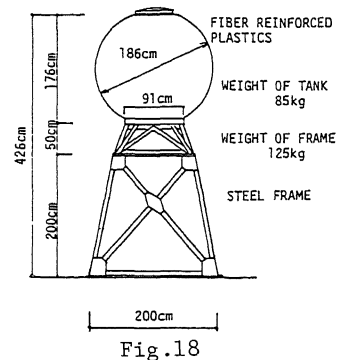


Fig.18

RECTANGULAR WATER TANK TEST

The small scale model of a water tank, shown in Fig.19, was experimented by using a small three dimensional shaking table. The side wall responses were measured by strain gages, pressure gages, and acceleration sensors. The response records of one dimensional random excitations for the X-, Y-, and Z-direction are shown in Fig.20 respectively. Fig.21 gives two kinds of records. The left hand side is the three dimensional excitation record, and the right hand side is the synthesized waves superposing one dimensional excitation records of the X-, Y-, and Z-direction. The superposed waves indicate, as a matter of facts, good agreements with the response waves of three dimensional excitation. The principle of superpositions for directions were verified experimentally.

According to strain records of a random excitation, the response waves caused by a first sloshing were deformed, as always measured. Responses at the center position of side walls parallel to the shaking direction indicated double frequencies of first sloshings. These nonlinear sloshing responses to random excitations were analyzed. Bernoulli theorem including second order of velocities, and kinematic boundary conditions of free surfaces were applied to this ansalsis. The velocity potential in the vicinity of free surfaces was developed in Taylor series, and concerning wave height, the terms more than three orders were neglected. The following equation was obtained,

$$\frac{\partial^2 \dot{\phi}}{\partial t^2} + g \frac{\partial \dot{\phi}}{\partial z} = \frac{\partial^2 \dot{\phi}}{\partial x^2} \frac{\partial \dot{\phi}}{\partial t} - 2 \frac{\partial \dot{\phi}}{\partial x} \frac{\partial^2 \dot{\phi}}{\partial t \partial x} \dots \text{Eq. (4)}$$

$$- \frac{\partial \dot{\phi}}{\partial z} \frac{\partial^2 \dot{\phi}}{\partial t \partial z} + \frac{1}{g} \left(\frac{\partial^2 \dot{\phi}}{\partial t^2} \frac{\partial^2 \dot{\phi}}{\partial t \partial z} + \frac{\partial \dot{\phi}}{\partial t} \frac{\partial^3 \dot{\phi}}{\partial t^2 \partial z} \right)$$

Assuming $\dot{\phi} = \dot{\phi}_1 + \dot{\phi}_2$, $\dot{\phi}_1$ is the linear sloshing potential as follow,

$$\dot{\phi}_1 = \sum_{m=1,2} \dot{\beta}_m \cos \frac{m\pi x}{a} \cosh \frac{m\pi}{a} z - \left(x - \frac{a}{2} \right) \dot{u}_g \dots \text{Eq. (5)}$$

where u_g is a input motion, a is the width of a tank. β_m was obtained by solving the linear sloshing equation. $\dot{\phi}_2$ was assumed as follow,

$$\dot{\phi}_2 = \sum_{n=1,2} \dot{\alpha}_n \cos \frac{n\pi x}{a} \cosh \frac{n\pi}{a} z \dots \text{Eq. (6)}$$

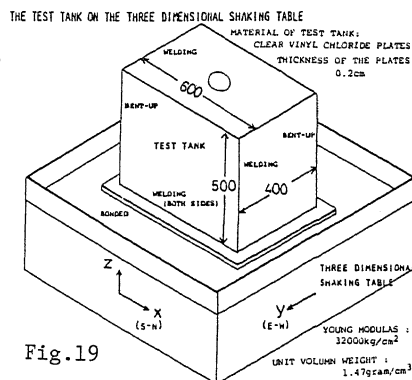


Fig.19

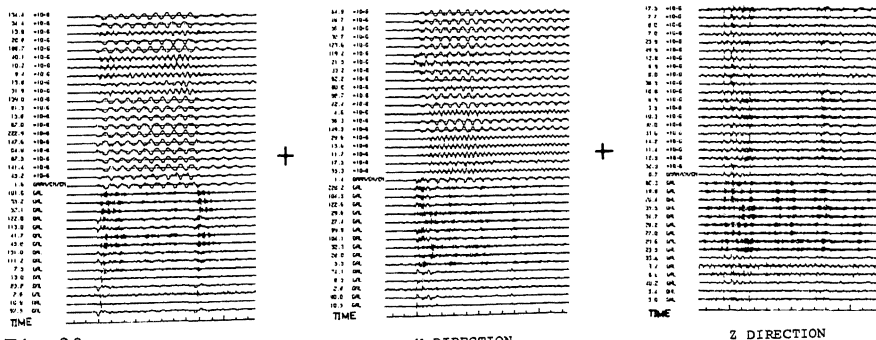


Fig.20 X DIRECTION

Y DIRECTION

Z DIRECTION

The linear solution ϕ_1 , was then fed back to the right-hand side of Eq(4) and the equations were solved again for the second order term ϕ_2 . So α_1 was obtained. In the case of solving for a first sloshing mode, only the second mode ($n=2$) of Eq.(6) was found. Fig.22 is the calculated wave height responses over free surfaces. The damping factors used for calculations were 0.1%. Using the perturbation methods like this procedure, the nonlinear sloshing responses of rectangular water tanks to earthquake waves are calculated easily.

CONCLUSIONS

The water tank of high-rise configurations makes horizontal responses including rocking motions. These rocking motions are something to do with anchor bolt connections. The vibration analyses considering rocking motions will be necessary for the water tanks of any configurations.

The walls of rectangular tanks have to be given sufficient rigidities by adding inner bracings and outer rib supports. However, if it is impossible to give sufficient rigidities, the wall must have enough ductilities, so as not to leak.

ACKNOWLEDGEMENTS

The author wishes to express his sincere gratitude to Dr. H. Shibata, Professor of the Institute of Industrial Science, Tokyo University, for his helpful suggestions

The author is grateful to SEKISUI KOJI CO., LTD., BRIDGE-STONE TIRE CO., LTD., and Messrs N. Ogawa, S. Nomura, H. Iida of National Research Center for Disaster Prevention, for their cooperations throughout experiments.

REFERENCIES

- Ref. 1 J.W. Miles, On the Sloshing of Liquid in a Flexible Tank, JOURNAL OF APPLIED MECHANICS, June 1958
 Ref. 2 M.A. Haroun, Dynamic Analyses of Liquid Storage Tanks, EERL 80-4, February 1980
 Ref. 3 B. Budiansky, Sloshing of Liquid in Circulat Canals and Spherical Tanks, Journal of the Aero/Space Sciences, March 1960
 Ref. 4 N. Shimizu, Proceedings of JSME NO. 800-12 page 69-71(in Japanese), August 1980

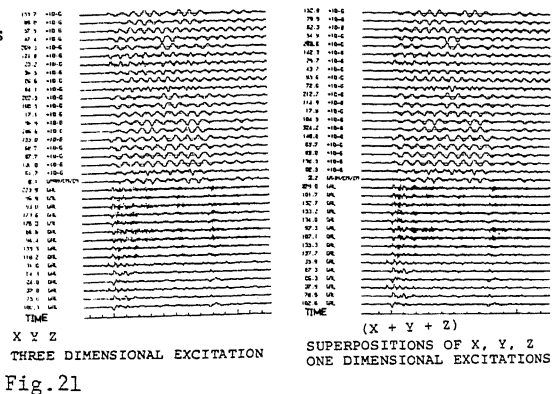


Fig.21

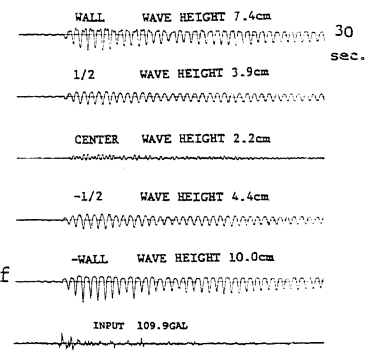


Fig.22 WAVE HEIGHT DISTRIBUTION